Published in final edited form as:
Curr Osteoporos Rep. 2013 June ; 11(2): 147–155. doi:10.1007/s11914-013-0142-7.

Clinical Imaging of Bone Microarchitecture with HR-pQCT

Kyle K. Nishiyama and **Elizabeth Shane**
Metabolic Bone Diseases Unit, Division of Endocrinology, Department of Medicine, College of Physicians and Surgeons, 630 West 168th Street, PH8 West 864, New York, NY 10032, USA

Abstract

Osteoporosis, a disease characterized by loss of bone mass and structural deterioration, is currently diagnosed by dual-energy x-ray absorptiometry (DXA). However, DXA does not provide information about bone microstructure, which is a key determinant of bone strength. Recent advances in imaging permit the assessment of bone microstructure in vivo using high-resolution peripheral quantitative computed tomography (HR-pQCT). From these data, novel image processing techniques can be applied to characterize bone quality and strength. To date, most HR-pQCT studies are cross-sectional comparing subjects with and without fracture. These studies have shown that HR-pQCT is capable of discriminating fracture status independent of DXA. Recent longitudinal studies present new challenges in terms of analyzing the same region of interest and multisite calibrations. Careful application of analysis techniques and educated clinical interpretation of HR-pQCT results have improved our understanding of various bone-related diseases and will no doubt continue to do so in the future.

Keywords

High-resolution peripheral quantitative computed tomography; HR-pQCT; Bone microarchitecture; Osteoporosis; Fragility fractures; Finite element analysis; Clinical imaging

Introduction

Osteoporosis is a serious degenerative disease characterized by both the loss of bone mass and the deterioration of bone architecture [1]. Current clinical diagnosis of osteoporosis relies on measurements of areal bone mineral density (aBMD) by dual-energy x-ray absorptiometry (DXA). While aBMD is a significant predictor of fracture risk [2], it is limited because of its two-dimensional nature, which is affected by the size and position of the subject [3] and cannot distinguish between the cortical and trabecular compartments. Epidemiological data indicate that over 80 % of fractures occur in women who would not be classified as osteoporotic according to current aBMD criteria [4], highlighting the limitations of this approach and the need for other assessment methods. Bone structure is fundamental to bone strength and, thus, in vivo structural information is critical for the assessment of disease progression, treatment effects, and risk of fracture [5].

E. Shane es54@columbia.edu.

Conflict of Interest K Nishiyama declares no conflicts of interest and E Shane declares no conflicts of interest.

Recent advances in medical imaging techniques allow bone structure to be assessed at various skeletal sites within the body. Three-dimensional macro- and microstructure of both the cortical and trabecular regions can be imaged non-invasively, which was previously possible only by quantitative histomorphometry of transiliac bone biopsies [6]. The primary tools for assessing volumetric density and bone structure are quantitative computed tomography (QCT) and more recently, high-resolution peripheral quantitative computed tomography (HR-pQCT). Central QCT has the advantage of being able to image the two main osteoporotic fracture sites: the proximal femur and spine at in plane-resolutions of approximately 200–500 μm [7], but these resolutions are not high enough to examine the trabecular and cortical microstructure. While HR-pQCT is restricted to peripheral sites such as the distal radius and distal tibia, it produces images with an isotropic voxel size of 82 μm, allowing for the measurement of bone microstructure. To date, the majority of these HR-pQCT scanners still exist in research environments but their use has dramatically increased since their introduction in 2005. Most of the published studies using HR-pQCT have focused on the technical aspects and validation but recently there has been a large increase in the number of studies demonstrating the clinical utility of HR-pQCT. This article reviews the ability of HR-pQCT to assess bone microarchitecture and highlights the results from recent clinical studies.

HR-pQCT Imaging

Image Acquisition and Processing

HR-pQCT acquires images based on the same principles as traditional QCT but can achieve a much higher resolution with the trade-off of a smaller field of view. This permits only the scanning of peripheral sites such as the radius and tibia. Scans take 2.8 minutes to acquire an axial 9.02 mm section in the only currently available commercial system (XtremeCT; Scanco Medical, Brüttisellen, Switzerland). Further technical details can be found elsewhere [8, 9]. A calibration phantom is scanned daily to accurately report hydroxyapatite bone mineral densities. Radiation exposure during an HR-pQCT scan is several orders of magnitude lower than whole body CT at an approximate 3 μSv effective patient dose per scan.

Prior to scan acquisition, the wrist or ankle is immobilized in a carbon cast that is fixed within the scan gantry. A projection image is acquired so that the operator can mark a reference line at the radial or tibial midjoint. The scan region of interest is 9.5 mm proximal to this reference line at the radius and 22.5 mm proximal to the tibia reference line. Other studies have defined varying scan regions [10] in particular for the study of children and adolescents [11–14]. This insures the growth plate is not exposed to radiation and accounts for differences in bone size.

The scanner acquires raw projection data that is reconstructed to generate a stack of two-dimensional gray-scale images. To evaluate the cortical and trabecular compartments separately, the regions must be segmented (Fig. 1). The standard manufacturer method uses a filter and threshold method to extract the cortical region [15]. Unfortunately, this method fails to extract the cortex when it is thin or highly porous [16, 17]. Recently, newer methods have been developed in conjunction with the manufacturer so that the cortical and trabecular

regions can be extracted automatically and permit measurement of cortical porosity and direct cortical thickness [17–19].

Density Analysis

Based on the pre-calibration of the system and the segmentation of the cortical and trabecular compartments, volumetric bone mineral density (vBMD, mg HA/cm^3) can be determined for the whole bone, trabecular bone (Tb.BMD), and cortical bone (Ct.BMD). Based on the grayscale images, tissue mineral density can also be calculated [20]. HR-pQCT images can also be used to simulate areal BMD measurements with a high level of agreement with ultradistal radius DXA measurements [21].

Trabecular Bone Structure Analysis

In addition to vBMD, bone morphometric analysis can be used to assess the microstructural properties of bone. However, since the resolution of HR-pQCT is relatively close to the size of individual trabeculae, trabecular measurements are generally derived rather than directly measured from the images [15]. The bone volume fraction (BV/TV, %) is determined from the trabecular vBMD assuming the density of fully mineralized bone is 1200 mg HA/cm^3. The average number of trabeculae (Tb.N, 1/mm) is directly measured using ridge extraction methods [22]. Average trabecular thickness (Tb.Th, mm) and separation (Tb.Sp, mm) are calculated using semi-derived methods (Tb.Th = (BV/TV)/Tb.N and Tb.Sp = (1-BV/TV)/Tb.N) [15].

In addition to the standard manufacturer analysis, additional customized analyses can be performed on the trabecular region. One of these methods is individual trabeculae segmentation (ITS) that assesses the orientation and the ratio of rod and plate trabecular elements, a determinant of bone strength [23]. Briefly, this method creates a skeleton of the trabecular region and classifies each trabecular element as a surface or curve, as described in detail elsewhere [24]. Other analysis metrics include connectivity, anisotropy, and structure model index [25]; however, these parameters may be more strongly affected by image resolution [26].

Trabecular bone HR-pQCT measurements are highly correlated with measurements performed on cadavers by micro-computed tomography (micro-CT) measurements [27, 28], but correlated moderately with iliac crest microstructure assessed by micro-CT and poorly with two-dimensional histomorphometry [29]. In addition, various precision studies have reported coefficient of variations for density and morphological parameters [30–34] one of which was the first multisite precision study [35].

Cortical Bone Structure Analysis

Since cortical thickness (Ct.Th) can be well resolved with HR-pQCT, it can be measured directly; however, depending on the compartment segmentation, derived Ct.Th measurements are also used. The direct measurement is based on a distance transform of the cortical region [22]. The derived measurement of Ct.Th is calculated as the volume of the cortical bone divided by outer bone surface [15]. Both the direct and derived measurements of cortical thickness have shown very good agreement with gold-standard micro-CT scans

of cadaver bones [17, 28]. Cortical porosity (Ct.Po) can also now be measured from HR-pQCT images. One of these methods uses an automatic segmentation [18] of the cortical and trabecular regions, binarizes the image, and then calculates the percentage of void voxels in the cortex from the total cortical voxels. This method has been validated for accuracy [17] and reproducibility [19] and is currently being distributed by the manufacturer (Scanco Medical). Another method has been proposed and patented [36], and uses density information to estimate pores that are too small to be directly measured. Density of each voxel is calculated as a percentage of fully mineralized bone (assumed to be 1200 mg HA/cm^3) to estimate the porosity.

Estimates of Bone Strength

Based on the HR-pQCT images, bone strength can be estimated using finite element (FE) analysis. The resolution is high enough that the structure can be represented directly by the elements in the model. FE models based on HR-pQCT images have been validated against micro-CT models [27] as well as mechanical testing [37]. Images can be binarized to all "bone" elements and assigned a homogenous elastic modulus. In specific applications where mineralization changes may be expected, models can incorporate tissue in homogeneities based on the x-ray attenuation values [38]. Due to the extremely large size of these models, custom FE solvers are required [37, 39]. Typically a uniaxial compression to 1 % strain is applied and whole bone stiffness (kN/mm) and failure load (N) are reported.

Clinical Applications

Age-, Sex-, and Race-Related Variation

Many of the initial studies demonstrating the clinical utility of HR-pQCT have focused on determining the age- and sex-related differences in bone microarchitecture. Boutroy and colleagues published the first cross-sectional study to report bone microarchitecture differences using HR-pQCT [30]. They compared pre- and postmenopausal women and those with osteoporosis and found significant differences in bone microarchitecture. The first population-based study using HR-pQCT to investigate the age-related variation in both men and women (n=602, ages 21–97 years) reported that decreases in BV/TV were similar between men and women but there were marked structural differences between the sexes at the distal radius [32]. While there were similar rates of age-related declines in BV/TV, in men it was related to thinning of the trabeculae, while in women there was a decrease in the number of trabeculae, which would have a much greater impact on bone strength. Dalzell and colleagues later confirmed the differences in the structural basis of bone loss between men and women at both the radius and tibia [40]. The most recent study to examine age- and sex-related variation with HR-pQCT is in a Canadian population-based sample (n=644, ages 20–99 years) that reported age-related bone loss differs not only between men and women but also between the cortical and trabecular compartments [41•]. Significant decreases in cortical bone density due to an increase in cortical porosity occurred with aging. There was an exponential increase in porosity that occurred around the time of menopause, supporting the theory that estrogen deficiency contributes to cortical bone loss. While these studies have elucidated some of the mechanisms underlying age-related bone loss, there is still a need for longitudinal studies with HR-pQCT to eliminate the possibility of secular trends.

Recent studies have also suggested that global analysis may be hiding some of the age-related differences in microstructure, and regional analysis of the radius and tibia may be valuable [42–44].

HR-pQCT has also been used to provide an in-depth analysis of bone growth in children and adolescents, groups particularly affected by the limitations of DXA due to bone size differences and bone growth [45]. A consistent findings of these studies is the detection of transient deficits in cortical bone during puberty [13, 46–48]. During this time of rapid growth, predominantly in boys, cortical bone consolidation lags behind; this transient deficit may partially account for the high incidence of fractures at this age. In contrast, however, a prospective study of 176 boys found that those with fractures had lower Tb.BMD, Tb.N, and FE estimates of bone strength but not Ct.BMD nor Ct.Th than fracture-free boys of the same age [49]. It is possible that during this time of high incidence of fracture, boys with trabecular architecture that sufficiently compensates for the deficit in cortical bone are less likely to fracture.

The apparent paradox that Asian women have lower aBMD than Caucasian women and also have lower fracture rates has been investigated with HR-pQCT. Two studies have found that Chinese women had denser, thicker cortices compared with Caucasian women, which may offset the strength disadvantage due to smaller bones in Chinese women [50, 51]. A recent study suggested more preferential loss of plate-like trabeculae in Chinese-American women compared with Caucasian women [52]. However, it appears the denser and thicker cortices compensate for this loss and it is possible that clinical management of Asians and Caucasians at risk of fracture should differ because of the compartment specific difference in bone loss.

Relationship to Fracture

To date, the majority of the clinical studies using HR-pQCT have examined associations with fracture, predominantly in postmenopausal women with osteopenia and osteoporosis [53–62, 63•, 64]. Two of the first studies examining bone microarchitecture and fracture found that bone structure contributes to fracture risk independently of aBMD highlighting the importance of the structural information [56, 57]. When comparing subjects with hip fracture to controls, BV/TV, Tb.N, Ct.Th, and Ct.BMD were significantly reduced in those with fracture and cortical parameters were significantly different between those with wrist fracture compared with those with hip fracture [59]. This provides some evidence that the severity of the bone deterioration is related to the cortical region. Stein and colleagues also compared postmenopausal women with (n=68) and without (n=101) previous fracture and found that those with fracture had reduced vBMD, more microarchitectural deterioration, and lower estimated bone strength by FE analysis; however, no measurement could adequately discriminate fracture status [60]. This suggests that combinations of parameters or advanced statistical techniques may be necessary to discriminate fractures.

Using principal component analysis (PCA), two studies [55, 58] have explored combinations of parameters to discriminate fracture status. With PCA, the components should separate into meaningful combinations of the variables. Both of these studies demonstrated that the first principal component, which accounts for the majority of the variance in the data, was

represented mainly by Ct.BMD, Ct.Th, and FE estimates of bone strength [55, 58] and was significantly associated with wrist fracture [58] and fractures at all sites [55]. Trabecular indices were generally accounted for in the second principal component, but did not result in significant odds ratios for fracture [55, 58]. While this study highlights the importance of cortical bone in determining bone strength, it is possible that the lack of association with the component representing trabecular indices was due to the small sample size of the study.

The severity of fractures has also been associated with bone microarchitecture, indicating it may be a more sensitive means of discriminating fractures than DXA. For both women [53] and men [65], cortical architecture was associated with the severity of vertebral fractures, and was independent of aBMD in both sexes. In addition, more severe microarchitectural abnormalities have been reported in postmenopausal women with vertebral fractures compared with those with nonvertebral fractures [63•].

Differences in bone microarchitecture between those with and without fracture have also been established in men [66–68]. The first study of men with fracture (n=185) compared with age-, height- and weight-matched controls by Vilayphiou et al. demonstrated that microarchitecture and FE estimates of strength were associated with all types of fractures [66]. Interestingly, both the radius and tibia were affected, suggesting that weight bearing at the tibia did not seem to preserve bone microstructure as it did in women [55]. Graeff et al. found that HR-pQCT microstructural measurements and FE estimates of bone strength were also superior to DXA in discriminating vertebral fracture status in men with glucocorticoid-induced osteoporosis [68].

Most recently, studies have used machine-learning algorithms to discriminate those with and without fracture. These classification methods are “trained” on a specific dataset then can be “tested” on another set. To classify subjects with and without previous fractures, gradient boosting machines [64] and support vector machines [61] have been used. Both methods achieved very high accuracies and areas under the receiver operating characteristic curves and also outperformed DXA at classifying subjects with fracture. While larger prospective studies are needed, these tools could eventually be used for fracture risk assessment and prediction.

Secondary Osteoporosis and Related Bone Diseases

Secondary causes of osteoporosis and related bone diseases have been an important area of HR-pQCT clinical applications, particularly because these diseases may affect the cortical and trabecular compartments differently. One such condition is primary hyperparathyroidism (PHPT), where it has long been suspected that cortical bone is negatively affected but the trabecular region is preserved. Hansen and colleagues compared patients with PHPT to age-matched, healthy controls in a cross-sectional study [69]. At the radius they found, as anticipated, lower Ct.Ar and Ct.Th, but contrary to expectations, they also found lower Tb.N and higher Tb.Sp in PHPT subjects compared with controls. These trends were not apparent at the tibia, possibly due to a small sample size. In a larger study, Stein et al. recently reported lower trabecular plate-to-rod ratios and lower numbers of trabecular junctions at both the tibia and radius in women with PHPT compared with

controls [70]. These results contrast with observations found by iliac crest biopsies, possibly indicating site-specific differences in the effects of PTH.

Hansen and colleagues also reported changes in microarchitecture one year after a parathyroidectomy, by which point Ct.BMD and Ct.Th either increased or was maintained at both radius and tibia, while at the radius there was also an increase in Tb.N and a decrease in Tb.Sp. In this longitudinal study, results should be carefully interpreted as this is a clinical situation in which there is trabecularization of the cortical bone. Large increases in cortical porosity may cause the region adjacent to the endocortical surface to be classified as trabecular bone, potentially improving the trabecular indices and confounding the cortical bone changes.

In patients with chronic kidney disease (CKD), HR-pQCT is a particularly promising tool because of the suspected effects on the cortical bone compartment. In addition, DXA is affected by vascular calcifications that may introduce errors in aBMD measurements. However, given the high probability of secondary hyperparathyroidism (SHPT) in patients with CKD, there are similar concerns regarding trabecularization of endocortical bone. Nickolas et al. compared CKD patients with and without fracture and found that those with fracture had lower Ct.Ar, Ct.Th, vBMD, and Tb.N at the distal radius as well as cortical deterioration at the distal tibia [71]. In terms of fracture discrimination, DXA and HR-pQCT individual parameters performed equally well; however, FE was not performed in this study and it is possible that FE estimates of bone strength or combinations of HR-pQCT parameters would better discriminate fracture status. Most recently it was reported that compared with controls, women with end-stage renal disease had more bone deterioration than men [72]; however, it is still unclear why this difference was observed and larger studies are needed to confirm this finding.

HR-pQCT has also been used to explain the reports of higher fracture incidence in patients with type II diabetes despite having normal aBMD. Affected patients had increased trabecular bone density but reduced cortical bone [73]; however, these results were not supported by another study by Shu et al. in which HR-pQCT parameters were similar between type II diabetics and healthy controls [74]. Both of these studies are limited by small numbers of subjects and Shu and colleagues did not examine cortical porosity. However, it is conceivable that patients with diabetes maintain normal aBMD but since the bone mass is redistributed from the cortical to the trabecular compartment, there is less resistance to bending and thus increased fracture risk. This is supported by a recent study that compared women with and without diabetes and those with and without fracture and found that deficits in cortical bone, particularly increased Ct.Po, were apparent in the postmenopausal diabetic women with fractures [75].

The clinically relevant information provided by HR-pQCT is highlighted by the recent array of applications to various populations. These include subjects with premenopausal idiopathic osteoporosis [24], osteogenesis imperfecta [76], and athletes with amenorrhea [77]. In all cases, significant differences in bone microarchitecture were found when compared with healthy controls. Visceral adipose tissue and bone marrow fat have been found to be negative predictors of bone microarchitecture [78], and after bariatric surgery, bone

microarchitectural changes reflected those occurring in hyperparathyroidism, with losses particularly concentrated in the cortical bone [79].

Monitoring Treatment Effects

In one of the first multicenter, randomized, placebo-controlled studies that applied HR-pQCT, the effects of denosumab and alendronate were compared after 12 months in 247 postmenopausal women [80•]. Compared with the placebo group, both treatments were found to prevent structural decay. However, with denosumab, there were significantly higher increases in total and cortical BMD compared with alendronate. The lack of significant changes in microstructural parameters in this study may be due to the variability introduced due to scanning at multiple centers and is an important challenge that must be addressed for future multi-site studies.

HR-pQCT has also been used to compare effects of alendronate and strontium ranelate in postmenopausal osteoporotic women [81, 82•]. At completion of the 24-month study [82•], tibia Ct.Th, Ct.BMD, and trabecular BV/TV increased with strontium ranelate but not with alendronate. At the radius, only Ct.BMD was higher in the strontium ranelate than the alendronate group. Importantly, these structural and density improvements with treatment were also captured by FE estimates of failure load. While it is not possible to quantify the effect that strontium may have on x-ray attenuation, it appears the improvements in Ct.Th provide an important advantage of strontium ranelate over alendronate treatment.

Burghardt and colleagues performed a pilot, placebo-controlled study with alendronate over 24 months [20]. In the alendronate group, there were improvements at the distal tibia only for cortical and trabecular BMD, as well as Ct.Ar, and Ct.Th, suggesting the changes were driven by endocortical and trabecular changes. In the most recent bisphosphonate trial, Chapurlat et al. performed a randomized placebo-controlled study of ibandronate in 148 osteopenic women [83]. Similar to the results reported by Burghardt et al. [20], changes with treatment were not observed at the radius, but at the tibia there were improvements in Ct.BMD and maintenance of Ct.Th after 12 and 24 months [83]. It is important to note that neither of these studies investigated the effects of bisphosphonates on the tissue mineral properties, which would likely also contribute to bone strength.

Furthermore, HR-pQCT has been used to determine the effects of teriparatide on bone microstructure and estimated strength [84–86]. In a small, 18-month longitudinal study, Macdonald et al. [86] found decreased total BMD at the distal radius and decreased Ct.BMD, increased Tb.Th and BV/TV at both the distal radius and distal tibia. There was a trend for increased Ct.Po and no detected change in bone strength estimates at either site. These non-significant changes may be explained both by the small sample size or the simplified axial compression of the FE analysis. Hansen and colleagues recently compared the effects of PTH 1–34, PTH 1–84, and zoledronic acid in an 18-month, open-label study [85]. Both PTH treatments increased Ct.Po at the radius and tibia, but also increased Tb.N at the tibia. Increases in Ct.Th were also observed at the radius with PTH 1–34. Zoledronic acid increased Ct.Th and Ct.BMD at the tibia and BV/TV at both sites. These results were consistent with previous reports that PTH may increase cortical remodeling with a net positive formation rate compared with resorption on the endocortical surface. Bone strength

estimates were preserved with PTH 1–34 and zoledronic acid but actually decreased with PTH 1–84 [85]. As the authors noted, this warrants further investigation, but in the future it may be important to use FE models that incorporate scaled material properties to account for changes in mineralization.

Conclusions

In the past decade, the technical and validation aspects of HR-pQCT have been established so that researchers can now explore the clinical utility of the device. This review has provided a brief overview of the scan acquisition and measurement capabilities and highlighted results of several recent studies that speak to the clinical applications of this technology.

Age- and sex-related differences have now been well documented for both adult and adolescent populations and initial studies have shown that fracture discrimination is improved when microstructure parameters are measured compared with DXA alone. An increasing number of studies have applied HR-pQCT to various bone diseases, which has been particularly useful in applications where the cortical and trabecular regions are affected differently. The first longitudinal treatment trials are beginning to be published and the application of HR-pQCT to understanding the effects of various bone active therapies will be a future area of progress.

Currently the number of devices available and the lack of standardization limit the widespread clinical use of HR-pQCT. While some multicenter studies have been completed, as well as multisite precision studies, there is still a need for further large-scale, comparative, and prospective studies. Despite these limitations, the use of HR-pQCT is extremely promising and will no doubt advance our understanding of bone quality and strength, and the effects of treatments with the ultimate goal of reducing fractures.

References

Papers of particular interest, published recently, have been highlighted as:

• Of importance

1. NIH Consensus Development Panel on Osteoporosis Prevention DAT. Osteoporosis prevention, diagnosis, and therapy. JAMA. 2001; 285:785–95. [PubMed: 11176917]
2. Kanis JA. Diagnosis of osteoporosis and assessment of fracture risk. Lancet. 2002; 359:1929–36. [PubMed: 12057569]
3. Bolotin HH. DXA in vivo BMD methodology: an erroneous and misleading research and clinical gauge of bone mineral status, bone fragility, and bone remodelling. Bone. 2007; 41:138–54. [PubMed: 17481978]
4. Stone KL, Seeley DG, Lui L, et al. BMD at multiple sites and risk of fracture of multiple types: long-term results from the study of osteoporotic fractures. J Bone Miner Res. 2003; 18:1947–54. [PubMed: 14606506]
5. Müller R, Rüegsegger P. Three-dimensional finite element modelling of non-invasively assessed trabecular bone structures. Med Eng Phys. 1995; 17:126–33. [PubMed: 7735642]
6. Parfitt AM, Drezner MK, Glorieux FH, et al. Bone histomorphometry: standardization of nomenclature, symbols, and units. Report of the ASBMR Histomorphometry Nomenclature Committee. J Bone Miner Res. 1987; 2:595–610. [PubMed: 3455637]

7. Rosen, C. Primer on the metabolic bone diseases and disorders of mineral metabolism. 7th ed. American Society of Bone and Mineral Research; Washington DC: 2009.
8. Krug R, Burghardt AJ, Majumdar S, Link TM. High-resolution imaging techniques for the assessment of osteoporosis. Radiol Clin N Am. 2010; 48:601–21. [PubMed: 20609895]
9. Burghardt AJ, Link TM, Majumdar S. High-resolution computed tomography for clinical imaging of bone microarchitecture. Clin Orthop Relat Res. 2011; 469:2179–93. [PubMed: 21344275]
10. Boyd SK. Site-specific variation of bone micro-architecture in the distal radius and tibia. J Clin Densitom. 2008; 11:424–30. [PubMed: 18280194]
11. Burrows M, Liu D, Moore S, McKay H. Bone microstructure at the distal tibia provides a strength advantage to males in late puberty: an hr-pqct study. J Bone Miner Res. 2010; 25:1423–32. [PubMed: 19874197]
12. Burrows M, Liu D, Perdios A, et al. Assessing bone microstructure at the distal radius in children and adolescents using hr-pqct: a methodological pilot study. J Clin Densitom. 2010; 13:451–5. [PubMed: 20663697]
13. Kirmani S, Christen D, van Lenthe GH, et al. Bone structure at the distal radius during adolescent growth. J Bone Miner Res. 2009; 24:1033–42. [PubMed: 19113916]
14. Liu D, Burrows M, Egeli D, McKay H. Site specificity of bone architecture between the distal radius and distal tibia in children and adolescents: an hr-pqct study. Calcif Tissue Int. 2010; 87:314–23. [PubMed: 20725826]
15. Laib A, Häuselmann HJ, Rüegsegger P. In vivo high resolution 3D-QCT of the human forearm. Technol Health Care. 1998; 6:329–37. [PubMed: 10100936]
16. Davis K, Burghardt A, Link T, Majumdar S. The effects of geometric and threshold definitions on cortical bone metrics assessed by in vivo high-resolution peripheral quantitative computed tomography. Calcif Tissue Int. 2007; 81:364–71. [PubMed: 17952361]
17. Nishiyama KK, Macdonald HM, Buie HR, Hanley DA, Boyd SK. Postmenopausal women with osteopenia have higher cortical porosity and thinner cortices at the distal radius and tibia than women with normal abmd: an in vivo hr-pqct study. J Bone Miner Res. 2010; 25:882–90. [PubMed: 19839766]
18. Buie HR, Campbell GM, Klinck RJ, MacNeil JA, Boyd SK. Automatic segmentation of cortical and trabecular compartments based on a dual threshold technique for in vivo micro-ct bone analysis. Bone. 2007; 41:505–15. [PubMed: 17693147]
19. Burghardt AJ, Buie HR, Laib A, Majumdar S, Boyd SK. Reproducibility of direct quantitative measures of cortical bone microarchitecture of the distal radius and tibia by hr-pqct. Bone. 2010; 47:519–28. [PubMed: 20561906]
20. Burghardt AJ, Kazakia GJ, Sode M, et al. A longitudinal hr-pqct study of alendronate treatment in postmenopausal women with low bone density: relations among density, cortical and trabecular microarchitecture, biomechanics, and bone turnover. J Bone Miner Res. 2010; 25:2558–71. [PubMed: 20564242]
21. Burghardt AJ, Kazakia GJ, Link TM, Majumdar S. Automated simulation of areal bone mineral density assessment in the distal radius from high-resolution peripheral quantitative computed tomography. Osteoporos Int. 2009; 20:2017–24. [PubMed: 19330422]
22. Hildebrand T, Rüegsegger P. A new method for the model-independent assessment of thickness in three-dimensional images. J Microsc. 1997; 185:67–75.
23. Liu XS, Sajda P, Saha PK, et al. Complete volumetric decomposition of individual trabecular plates and rods and its morphological correlations with anisotropic elastic moduli in human trabecular bone. J Bone Miner Res. 2007; 23:223–35. [PubMed: 17907921]
24. Liu XS, Cohen A, Shane E, et al. Individual trabeculae segmentation (ITS)—based morphological analysis of high-resolution peripheral quantitative computed tomography images detects abnormal trabecular plate and rod microarchitecture in premenopausal women with idiopathic osteoporosis. J Bone Miner Res. 2010; 25:1496–505. [PubMed: 20200967]
25. Hildebrand T, Rüegsigger P. Quantification of bone microarchitecture with the structure model index. Comput Methods Biomech Biomed Eng. 1997; 1:15–23.
26. Sode M, Burghardt AJ, Nissenson RA. Majumdar S. Resolution dependence of the non-metric trabecular structure indices. Bone. 2008; 42:728–36. [PubMed: 18276202]

27. Liu XS, Zhang XH, Sekhon KK, et al. High-resolution peripheral quantitative computed tomography can assess microstructural and mechanical properties of human distal tibial bone. J Bone Miner Res. 2010; 25:746–56. [PubMed: 19775199]

28. MacNeil JA, Boyd SK. Accuracy of high-resolution peripheral quantitative computed tomography for measurement of bone quality. Med Eng Phys. 2007; 29:1096–105. [PubMed: 17229586]

29. Cohen A, Dempster DW, Müller R, et al. Assessment of trabecular and cortical architecture and mechanical competence of bone by high-resolution peripheral computed tomography: comparison with transiliac bone biopsy. Osteoporos Int. 2010; 21:263–73. [PubMed: 19455271]

30. Boutroy S, Bouxsein ML, Munoz F, Delmas PD. In vivo assessment of trabecular bone microarchitecture by high-resolution peripheral quantitative computed tomography. J Clin Endocrinol Metab. 2005; 90:6508–15. [PubMed: 16189253]

31. Kazakia GJ, Hyun B, Burghardt AJ, et al. In vivo determination of bone structure in postmenopausal women: a comparison of hr-pqct and high-field MR imaging. J Bone Miner Res. 2007; 23:463–74. [PubMed: 18052756]

32. Khosla S, Riggs BL, Atkinson EJ, et al. Effects of sex and age on bone microstructure at the ultradistal radius: a population-based noninvasive in vivo assessment. J Bone Miner Res. 2006; 21:124–31. [PubMed: 16355281]

33. MacNeil JA, Boyd SK. Improved reproducibility of high-resolution peripheral quantitative computed tomography for measurement of bone quality. Med Eng Phys. 2008; 30:792–9. [PubMed: 18164643]

34. Mueller TL, Stauber M, Kohler T, et al. Non-invasive bone competence analysis by high-resolution pqct: an in vitro reproducibility study on structural and mechanical properties at the human radius. Bone. 2009; 44:364–71. [PubMed: 19027092]

35. Burghardt AJ, Pialat JB, Kazakia GJ, et al. Multi-center precision of cortical and trabecular bone quality measures assessed by HR-PQCT. J Bone Miner Res. 2012; 28:524–36. [PubMed: 23074145]

36. Zebaze, R.; Seeman, E.; Mbala, A., et al. Patent: method and system for image analysis of selected tissue structures. 2011. WO/2011/029153

37. MacNeil JA, Boyd SK. Bone strength at the distal radius can be estimated from high-resolution peripheral quantitative computed tomography and the finite element method. Bone. 2008; 42:1203–13. [PubMed: 18358799]

38. Bourne BC, van Der Meulen MCH. Finite element models predict cancellous apparent modulus when tissue modulus is scaled from specimen ct-attenuation. J Biomech. 2004; 37:613–22. [PubMed: 15046990]

39. Van Rietbergen B, Weinans H, Huiskes R, Odgaard A. A new method to determine trabecular bone elastic properties and loading using micromechanical finite-element models. J Biomech. 1995; 28:69–81. [PubMed: 7852443]

40. Dalzell N, Kaptoge S, Morris N, et al. Bone micro-architecture and determinants of strength in the radius and tibia: age-related changes in a population-based study of normal adults measured with high-resolution pqct. Osteoporos Int. 2009; 20:1683–94. [PubMed: 19152051]

41•. Macdonald HM, Nishiyama KK, Kang J, Hanley DA, Boyd SK. Age-related patterns of trabecular and cortical bone loss differ between sexes and skeletal sites: a population-based hr-pqct study. J Bone Miner Res. 2011; 26:50–62. [PubMed: 20593413] Population-based study of 644 men and women with HR-pQCT and FEA highlighting the site- and sex-specific differences in age-related bone loss. Women had less periosteal expansion, more porous cortices, and greater load on cortex, which may underpin the sex differences in fracture risk.

42. Sode M, Burghardt AJ, Kazakia GJ, Link TM, Majumdar S. Regional variations of gender-specific and age-related differences in trabecular bone structure of the distal radius and tibia. Bone. 2010; 46:1652–60. [PubMed: 20188877]

43. Kazakia GJ, Nirody JA, Bernstein G, et al. Age- and gender-related differences in cortical geometry and microstructure: improved sensitivity by regional analysis. Bone. 2013; 52:623–31. [PubMed: 23142360]

44. Schnackenburg KE, Macdonald HM, Ferber R, Wiley JP, Boyd SK. Bone quality and muscle strength in female athletes with lower limb stress fractures. Med Sci Sports Exerc. 2011; 43:2110–9. [PubMed: 21552163]
45. Binkovitz LA, Henwood MJ, Sparke P. Pediatric DXA: technique, interpretation and clinical applications. Pediatr Radiol. 2008; 38(Suppl 2):S227–39. Suppl 2. [PubMed: 18401617]
46. Wang Q, Wang XF, Iuliano-Burns S, et al. Rapid growth produces transient cortical weakness. A risk factor for metaphyseal fractures during puberty. J Bone Miner Res. 2010; 25:1521–6. [PubMed: 20200962]
47. Nishiyama KK, Macdonald HM, Moore SA, et al. Cortical porosity is higher in boys compared with girls at the distal radius and distal tibia during pubertal growth: an hr-pqct study. J Bone Miner Res. 2011; 27:273–82. [PubMed: 22028110]
48. Walsh JS, Paggiosi MA, Eastell R. Cortical consolidation of the radius and tibia in young men and women. J Clin Endocrinol Metab. 2012; 97:3342–8. [PubMed: 22761460]
49. Chevalley T, Bonjour JP, van Rietbergen B, Ferrari S, Rizzoli R. Fractures during childhood and adolescence in healthy boys: relation with bone mass, microstructure, and strength. J Clin Endocrinol Metab. 2011; 96:3134–42. [PubMed: 21795454]
50. Wang XF, Wang Q, Ghasem-Zadeh A, et al. Differences in macro- and microarchitecture of the appendicular skeleton in young Chinese and White women. J Bone Miner Res. 2009; 24:1946–52. [PubMed: 19459783]
51. Walker MD, Liu XS, Stein E, et al. Differences in bone microarchitecture between postmenopausal Chinese-American and White women. J Bone Miner Res. 2011; 26:1392–8. [PubMed: 21305606]
52. Walker MD, Liu XS, Zhou B, et al. Pre- and postmenopausal differences in bone microstructure and mechanical competence in Chinese-American and White women. J Bone Miner Res. 2013 doi: 10.1002/jbmr.1860.
53. Sornay-Rendu E, Cabrera-Bravo JL, Boutroy S, Munoz F, Delmas PD. Severity of vertebral fractures is associated with alterations of cortical architecture in postmenopausal women. J Bone Miner Res. 2009; 24:737–43. [PubMed: 19113929]
54. Melton LJ, Riggs BL, Keaveny TM, et al. Relation of vertebral deformities to bone density, structure, and strength. J Bone Miner Res. 2010; 25:1922–30. [PubMed: 20533526]
55. Vilayphiou N, Boutroy S, Sornay-Rendu E, et al. Finite element analysis performed on radius and tibia hr-pqct images and fragility fractures at all sites in postmenopausal women. Bone. 2010; 46:1030–7. [PubMed: 20044044]
56. Sornay-Rendu E, Boutroy S, Munoz F, Delmas PD. Alterations of cortical and trabecular architecture are associated with fractures in postmenopausal women, partially independent of decreased BMD measured by DXA: the OFELY study. J Bone Miner Res. 2007; 22:425–33. [PubMed: 17181395]
57. Melton LJ, Riggs BL, van Lenthe GH, et al. Contribution of in vivo structural measurements and load/strength ratios to the determination of forearm fracture risk in postmenopausal women. J Bone Miner Res. 2007; 22:1442–8. [PubMed: 17539738]
58. Boutroy S, Van Rietbergen B, Sornay-Rendu E, et al. Finite element analysis based on in vivo hr-pqct images of the distal radius is associated with wrist fracture in postmenopausal women. J Bone Miner Res. 2008; 23:392–9. [PubMed: 17997712]
59. Vico L, Zouch M, Amirouche A, et al. High-resolution pqct analysis at the distal radius and tibia discriminates patients with recent wrist and femoral neck fractures. J Bone Miner Res. 2008; 23:1741–50. [PubMed: 18665795]
60. Stein EM, Liu XS, Nickolas TL, et al. Abnormal microarchitecture and reduced stiffness at the radius and tibia in postmenopausal women with fractures. J Bone Miner Res. 2010; 25:2572–81. [PubMed: 20564238]
61. Nishiyama K, Macdonald M, Hanley A, Boyd K. Women with previous fragility fractures can be classified based on bone microarchitecture and finite element analysis measured with hr-pqct. Osteoporos Int. 2012 doi:10.1007/s00198-012-2160-1.
62. Liu XS, Stein EM, Zhou B, et al. Individual trabecula segmentation (ITS)-based morphological analyses and microfinite element analysis of hr-pqct images discriminate postmenopausal fragility

fractures independent of DXA measurements. J Bone Miner Res. 2012; 27:263–72. [PubMed: 22072446]

63•. Stein EM, Liu XS, Nickolas TL, et al. Microarchitectural abnormalities are more severe in postmenopausal women with vertebral compared with nonvertebral fractures. J Clin Endocrinol Metab. 2012; 97:E1918–26. [PubMed: 22821893] Women with and without fracture were compared and microarchitecture parameters and novel ITS measurements by HR-pQCT discriminated the fracture status independently of aBMD by DXA.

64. Atkinson EJ, Therneau TM, Melton LJ, et al. Assessing fracture risk using gradient boosting machine (GBM) models. J Bone Miner Res. 2012; 27:1397–404.

65. Szulc P, Boutroy S, Vilayphiou N, et al. Cross-sectional analysis of the association between fragility fractures and bone microarchitecture in older men: the STRAMBO study. J Bone Miner Res. 2011; 26:1358–67. [PubMed: 21611974]

66. Vilayphiou N, Boutroy S, Szulc P, et al. Finite element analysis performed on radius and tibia hr-pqct images and fragility fractures at all sites in men. J Bone Miner Res. 2011; 26:965–73. [PubMed: 21541999]

67. Ostertag A, Collet C, Chappard C, et al. A case–control study of fractures in men with idiopathic osteoporosis: fractures are associated with older age and low cortical bone density. Bone. 2013; 52:48–55. [PubMed: 23010106]

68. Graeff C, Marin F, Petto H, et al. High resolution quantitative computed tomography-based assessment of trabecular microstructure and strength estimates by finite-element analysis of the spine, but not DXA, reflects vertebral fracture status in men with glucocorticoid-induced osteoporosis. Bone. 2013; 52:568–77. [PubMed: 23149277]

69. Hansen S, Beck Jensen J-E, Rasmussen L, Hauge EM, Brixen K. Effects on bone geometry, density, and microarchitecture in the distal radius but not the tibia in women with primary hyperparathyroidism: a case–control study using hr-pqct. J Bone Miner Res. 2010; 25:1941–7. [PubMed: 20499376]

70. Stein EM, Silva BC, Boutroy S, et al. Primary hyperparathyroidism is associated with abnormal cortical and trabecular microstructure and reduced bone stiffness in postmenopausal women. J Bone Miner Res. 2012 doi:10.1002/jbmr.1841.

71. Nickolas TL, Stein E, Cohen A, et al. Bone mass and microarchitecture in CKD patients with fracture. J Am Soc Nephrol. 2010; 21:1371–80. [PubMed: 20395370]

72. Trombetti A, Stoermann C, Chevalley T, et al. Alterations of bone microstructure and strength in end-stage renal failure. Osteoporos Int. 2012 doi:10.1007/s00198-012-2133-4.

73. Burghardt AJ, Issever AS, Schwartz AV, et al. High-resolution peripheral quantitative computed tomographic imaging of cortical and trabecular bone microarchitecture in patients with type 2 diabetes mellitus. J Clin Endocrinol Metab. 2010; 95:5045–55. [PubMed: 20719835]

74. Shu A, Yin MT, Stein E, et al. Bone structure and turnover in type 2 diabetes mellitus. Osteoporos Int. 2011; 23:635–41. [PubMed: 21424265]

75. Patsch JM, Burghardt AJ, Yap SP, et al. Increased cortical porosity in type-2 diabetic postmenopausal women with fragility fractures. J Bone Miner Res. 2012; 28:313–24. [PubMed: 22991256]

76. Folkestad L, Hald JD, Hansen S, et al. Bone geometry, density, and microarchitecture in the distal radius and tibia in adults with osteogenesis imperfecta type I assessed by high-resolution pqct. J Bone Miner Res. 2012; 27:1405–12. [PubMed: 22407910]

77. Ackerman KE, Nazem T, Chapko D, et al. Bone microarchitecture is impaired in adolescent amenorrheic athletes compared with eumenorrheic athletes and nonathletic controls. J Clin Endocrinol Metab. 2011; 96:3123–33. [PubMed: 21816790]

78. Bredella MA, Lin E, Gerweck AV, et al. Determinants of bone microarchitecture and mechanical properties in obese men. J Clin Endocrinol Metab. 2012; 97:4115–22. [PubMed: 22933540]

79. Stein EM, Carrelli A, Young P, et al. Bariatric surgery results in cortical bone loss. J Clin Endocrinol Metab. 2013; 98:514–9.

80•. Seeman E, Delmas PD, Hanley DA, et al. Microarchitectural deterioration of cortical and trabecular bone: differing effects of denosumab and alendronate. J Bone Miner Res. 2010; 25:1886–94. [PubMed: 20222106] Double-blind, multisite longitudinal study with alendronate

and denosumab treated patients found microarchitecture parameters by HR-pQCT declined in the placebo group while alendronate prevented the decline and denosumab prevented decline or improved the structure.

81. Rizzoli R, Laroche M, Krieg MA, et al. Strontium ranelate and alendronate have differing effects on distal tibia bone microstructure in women with osteoporosis. Rheumatol Int. 2010; 30:1341–8. [PubMed: 20512336]

82•. Rizzoli R, Chapurlat RD, Laroche JM, et al. Effects of strontium ranelate and alendronate on bone microstructure in women with osteoporosis. Results of a 2-year study. Osteoporos Int. 2012; 23:305–15. [PubMed: 21909729] Randomized double-blind trial of strontium ranelate and alendronate and HR-pQCT outcomes. With strontium ranelate there was an increase in Ct.Th, Ct.BMD, and BV/TV at the tibia while alendronate maintained bone microstructure.

83. Chapurlat RD, Laroche M, Thomas T, et al. Effect of oral monthly ibandronate on bone microarchitecture in women with osteopeniaa randomized placebo-controlled trial. Osteoporos Int. 2013; 24:311–20. [PubMed: 22402673]

84. Chavassieux P, Karsdal MA, Segovia-Silvestre T, et al. Mechanisms of the anabolic effects of teriparatide on bone: insight from the treatment of a patient with pycnodysostosis. J Bone Miner Res. 2008; 23:1076–83. [PubMed: 18302508]

85. Hansen S, Hauge EM, Jensen J-EB, Brixen K. Differing effects of PTH 1–34, PTH 1–84 and zoledronic acid on bone microarchitecture and estimated strength in postmenopausal women with osteoporosis. An 18 month open-labeled observational study using hr-pqct. J Bone Miner Res. 2012 doi:10.1002/jbmr.1784.

86. Macdonald HM, Nishiyama KK, Hanley DA, Boyd SK. Changes in trabecular and cortical bone microarchitecture at peripheral sites associated with 18 months of teriparatide therapy in postmenopausal women with osteoporosis. Osteoporos Int. 2010; 22:357–62. [PubMed: 20458576]

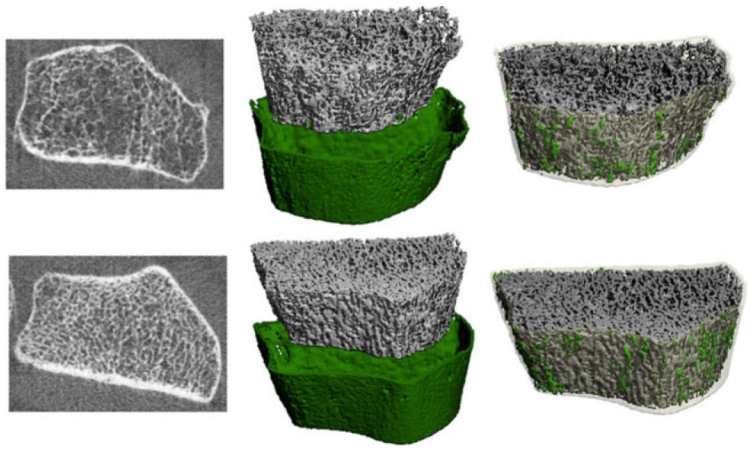

Fig. 1.

HR-pQCT images of the left radius of an individual who suffered a low-trauma fracture at the right radius (top row) and a fracture-free, age-matched control (bottom row). Figure depicts two-dimensional grayscale slices, the cortical and trabecular compartments segmented, and a three-dimensional rendering where cortical porosity is highlighted in green